CHEMISTRY
A EUROPEAN JOURNAL

FULL PAPER

DOI: 10.1002/chem.201203297

Isostructural Metal–Organic Frameworks Assembled from Functionalized Diisophthalate Ligands through a Ligand-Truncation Strategy

Yangyang Liu, Jian-Rong Li, Wolfgang M. Verdegaal, Tian-Fu Liu, and Hong-Cai Zhou*[a]

Abstract: Four isostructural metal–organic frameworks (MOFs) with various functionalized pore surfaces were synthesized from a series of diisophthalate ligands. These MOFs exhibit a new network topology of $\{4.6^4.8\}_2\{4^2.6^4\}\{6^4.8^2\}_2\{6^6\}$. Hydrogen uptake as high as 2.67 wt% at 77 K/1 bar and CO_2 uptake of 15.4 wt% at 297 K/1 bar have been observed for PCN-308, which contains $-CF_3$ groups. The isostructural series of MOFs also showed reasonable adsorption selectivity of CO_2 over CH_4 and N_2.

Keywords: adsorption · carbon dioxide · hydrogen storage · metal–organic frameworks · porous materials

Introduction

Rapid growth of CO_2 emission is considered one of the main causes of global climate change. CO_2 capture from flue-gas streams in fossil-fuel-fired power plants is becoming an urgent goal in environmental protection. Metal–organic frameworks (MOFs), which have emerged as a new class of porous materials, have great potential in this regard.[1] They are highly crystalline inorganic–organic hybrid materials that combine organic linkers and metal ions or metal-containing units.[2] Through the judicious selection of the inorganic and organic components, the structure and properties of MOFs can be systematically tuned on the atomic level. This endows the material with great advantages over other porous materials with large surface area, adjustable composition, and modifiable pore surfaces, size, and shape. For instance, coordinatively unsaturated metal centers (UMCs), which are often generated from the removal of terminally coordinated solvent molecules to the metal centers, can enhance gas adsorption and can also be utilized as Lewis acids for catalysis.[3] Moreover, the pore size and properties of the MOFs can be tailored by the choice of appropriate linkers with various functionalities as well as by postsynthetic modifications.[4] Another strategy to reduce CO_2 emission is to utilize clean-energy carriers such as hydrogen, which generates water as the only byproduct after energy is released. Hydrogen can be produced from renewable energy sources and has the highest gravimetric energy density of common fuels owing to its low molecular weight. However, owing to its extremely low volumetric energy density, the lack of an efficient means of storage is the major huddle that limits the practical use of hydrogen as a new energy carrier.[5] As new adsorbent materials with high porosity, MOFs are also promising storage media for hydrogen.[6]

Some MOFs have shown impressive CO_2-adsorption capacity and selectivity by incorporating specific functional groups or unsaturated open metal sites into the robust 3D framework. In particular, owing to the acidity of CO_2, some basic functional groups such as amine or amide groups in the organic ligands can help enhance CO_2 adsorption.[7] A pyridyl group is another basic functional group, but its effect on CO_2 adsorption in MOFs has rarely been studied. Polar functional groups such as the $-CF_3$ group were postsynthetically introduced to a zinc MOF and the modified MOF was found to have higher CO_2/N_2 selectivity, although postsynthetic modification decreased the surface area.[8] $[Cu(bpy\text{-}1)_2(SiF_6)]$ (bpy-1 = 4,4′-bipyridine) exhibits the highest CO_2 uptake and highest CO_2/CH_4 selectivity at 298 K and 1 atm among porous coordination polymers (PCPs) that do not contain open metal sites, although more studies are needed to address the effect of SiF_6^{2-} moieties.[9] Another MOF with a perfluorinated pore surface was found to be a promising material for hydrogen storage.[10] Functional groups, however, do not always have obvious effects on the gas-sorption properties of MOFs.[11] To systematically study the effects of various functional groups on gas-sorption properties of MOFs, ligands with pyridyl, methyl, and perfluoromethyl groups have been prepared in this work.

In MOF synthesis, symmetrically substituted organic linkers are usually preferred because MOFs based on these ligands tend to crystallize in space groups with high symmetry, which often facilitate crystallization and the subsequent crystallographic studies.[12] In addition, the synthesis of a symmetrical ligand tends to proceed with less complication.[13] Indeed, symmetrical linker extension is a general method to synthesize new MOFs that bear the same net-

[a] Y. Liu, Dr. J.-R. Li, W. M. Verdegaal, T.-F. Liu, Prof. H.-C. Zhou
Department of Chemistry, Texas A&M University
College Station, TX 77843 (USA)
Fax: (+1) 979-845-1595
E-mail: zhou@tamu.edu

Supporting information for this article is available on the WWW under http://dx.doi.org/10.1002/chem.201203297.

work topology[13,14] as the nonextended frameworks, and occasionally even entirely new structures.[12,15] Robust non-interpenetrated frameworks with extended ligands usually possess higher surface area[13] but extended linkers might also result in framework interpenetration[16] or collapse[17] during activation. The reverse of linker extension is ligand truncation (Scheme 1). This proposed strategy provides a method to introduce new types of building blocks with reduced symmetry, and the obtained frameworks might possess new topologies and interesting properties.

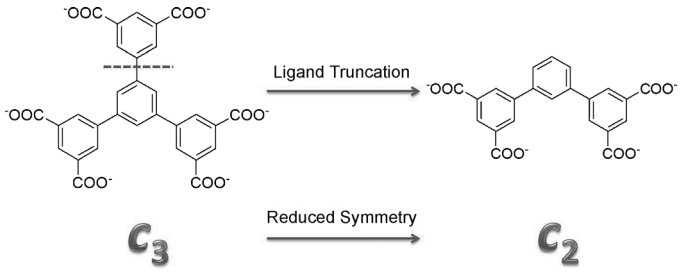

Scheme 1. Reduced symmetry ligand derived from the "ligand truncation" strategy.

Results and Discussion

Syntheses and structural characterizations: A series of C_2-symmetric ligands with different functional groups have been designed based on the "ligand truncation" strategy and synthesized by means of a Suzuki reaction. [1,1′:3′,1″-terphenyl]-3,3″,5,5″-tetracarboxylic acid (H_4TPTA) was obtained through the reaction between 1,3-dibromobenzene and diethyl 5-(4,4,5,5-tetramethyl-1,3,2-dioxaborolan-2-yl)-isophthalate followed by hydrolysis (for details on ligand synthesis, see the Experimental Section). 5,5′-(Pyridine-3,5-diyl)diisophthalic acid (H_4PDDA), 5′-(trifluoromethyl)-[1,1′:3′,1″-terphenyl]-3,3″,5,5″-tetracarboxylic acid (H_4FTPTA), and 5′-methyl-[1,1′:3′,1″-terphenyl]-3,3″,5,5″-tetracarboxylic acid (H_4MTPTA) were synthesized through the same method by simply changing the starting materials in the Suzuki reaction.

H_4PDDA contains two isophthalate groups and one pyridyl group. Solvothermal reaction between H_4PDDA and $Cu(NO_3)_2{\cdot}2.5\,H_2O$ in dimethylacetamide (DMA) solvent with tetrafluoroboric acid (HBF_4; 48% w/w aqueous solution) afforded green crystals of PCN-305 (PCN stands for "porous coordination network"). PCN-305 crystallizes in the orthorhombic *Cmcm* space group with $a=24.650(7)$, $b=33.494(9)$, $c=18.529(5)$ Å. Unlike most MOFs that consist of isophthalate moieties, PCN-305 does not contain cuboctahedral supramolecular building units in the structure.[18] Instead, there are one-dimensional channels along the *c* axis and the uncoordinated free pyridyl functional groups point to the pores of the framework (Figure 1a). The free volume

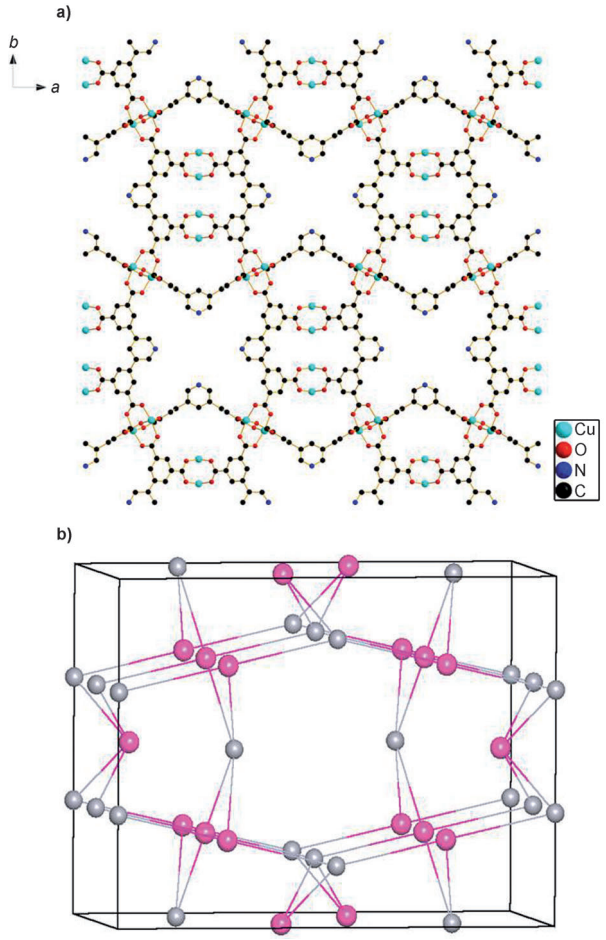

Figure 1. a) Structure of PCN-305 viewed along the *c* axis with the pyridyl groups pointing towards the pores. b) Topology of PCN-305.

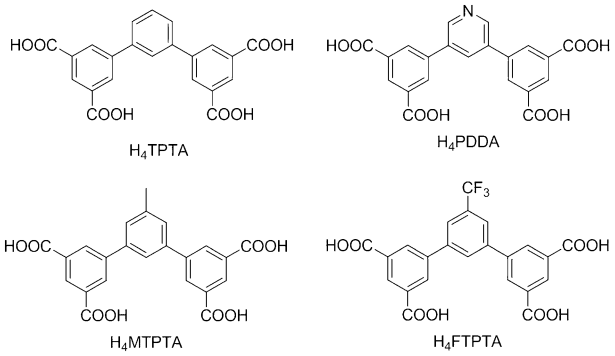

in fully desolvated PCN-305 is 69.8% as calculated by PLATON.[19] From the viewpoint of topology, the dicopper(II) paddlewheel secondary building units (SBUs) and PDDA ligands both serve as four-connected (4-c) nodes. As a result, PCN-305 adopts the very rare 4- 4-nodal net (Figure 1b) with a topological point symbol of $\{4.6^4.8\}_2\{4^2.6^4\}$-$\{6^4.8^2\}_2\{6^6\}$, which is previously unreported.

Isostructural MOFs PCN-306, -307, and -308 have been obtained from solvothermal reactions of $Cu(NO_3)_2{\cdot}2.5\,H_2O$ with H_4TPTA, H_4MTPTA, and H_4FTPTA, respectively, in *N*,*N*-dimethylformamide (DMF) solvent in the presence of

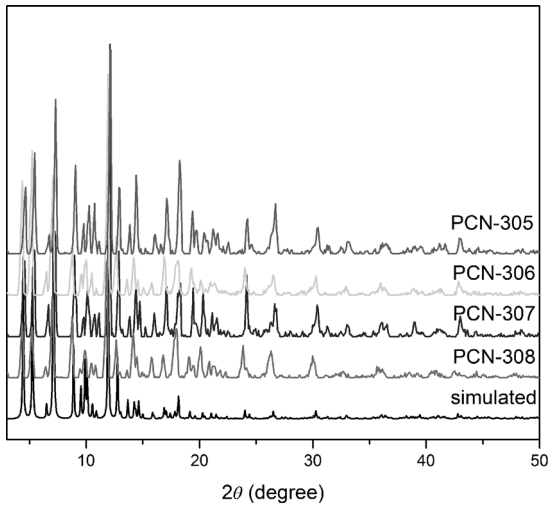

Figure 2. PXRD of isostructural MOFs PCN-305, -306, -307, and -308.

HBF_4. Powder X-ray diffractions (PXRD) shown in Figure 2 confirm they are isostructural. Thermal gravimetric analyses showed these four MOFs have similar thermal stability and decompose at around 300 °C (Figure S1 in the Supporting Information).

N_2 adsorption: The permanent porosity of the isostructural MOFs was confirmed by N_2 adsorption measurements at 77 K (Figure 3). PCN-305, -306, -307, and -308 were activated through the same procedure in which they were degassed under dynamic vacuum at 50 °C for 8 h after solvent exchange with methanol and then dichloromethane for two days each. Crystallinity of the MOFs is retained after the removal of solvent guest molecules, as indicated by the powder X-ray diffraction patterns (Figures S2–S5 in the Supporting Information).

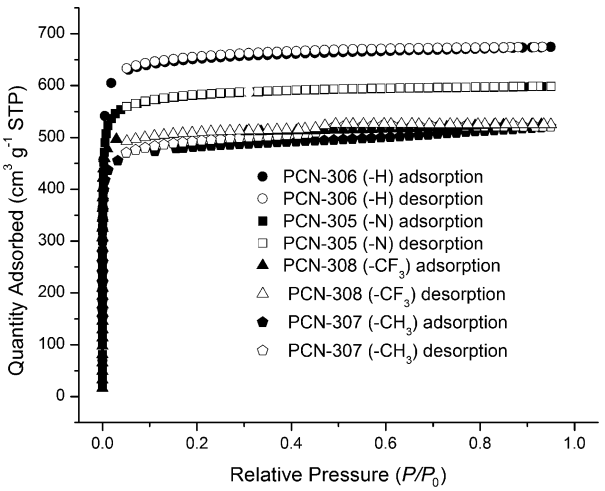

Figure 3. N_2-sorption isotherms of PCN-305, -306, -307, and -308 at 77 K.

A color change from green to deep purple-blue was observed, thus indicating the generation of open copper sites, which is typical for dicopper(II) paddlewheel frameworks.[20] The N_2 sorption for these isostructural MOFs at 77 K exhibits reversible type I isotherms, thus indicating their microporous nature. The calculated Brunauer–Emmett–Teller (BET) and Langmuir surface areas as well as pore volumes are listed in Table 1. Among them, PCN-306 with no functional groups has the highest surface area (BET: 1927 $m^2 g^{-1}$; Langmuir: 2929 $m^2 g^{-1}$) and pore volume (1.043 $cm^3 g^{-1}$). The surface area of PCN-305 is smaller than that of PCN-306. When adding $-CH_3$ or $-CF_3$ functional groups into the ligands, the surface areas and pore volumes of the MOFs understandably further decreased.

Table 1. Surface areas and pore volume of the isostructural MOFs.

MOF	S_{BET} [$m^2 g^{-1}$]	$S_{Langmuir}$ [$m^2 g^{-1}$]	V_{pore} [$cm^3 g^{-1}$]
PCN-306 (−H)	1927	2929	1.043
PCN-305 (−N)	1720	2599	0.926
PCN-308 ($-CF_3$)	1418	2234	0.810
PCN-307 ($-CH_3$)	1376	2235	0.808

$CO_2/CH_4/N_2$ gas adsorption: The CO_2, CH_4, and N_2 adsorptions at 273 K were measured for isostructural MOFs PCN-305, -306, -307, and -308 as shown in Figure 4. They exhibited impressive CO_2-adsorption capacity, particularly for PCN-308 with polar functional groups, among the highest reported so far. The CO_2 capacities for the isostructural MOFs at 273 and 297 K are listed in Table 2. Table 3 lists all the MOFs that have higher CO_2 adsorption capacities than PCN-308. From this we can see that PCN-308 has the same CO_2 capacity as the *N,N′*-dimethylethylenediamine (mmen)-incorporated MOF, mmen–CuBTTri (BTTri = 1,3,5-tris(1*H*-1,2,3-triazol-4-yl)benzene),[7f] although mmen–CuBTTri has a much higher heat of adsorption (96 kJ mol^{-1}). This can be attributed to the higher surface area of PCN-308 (BET sur-

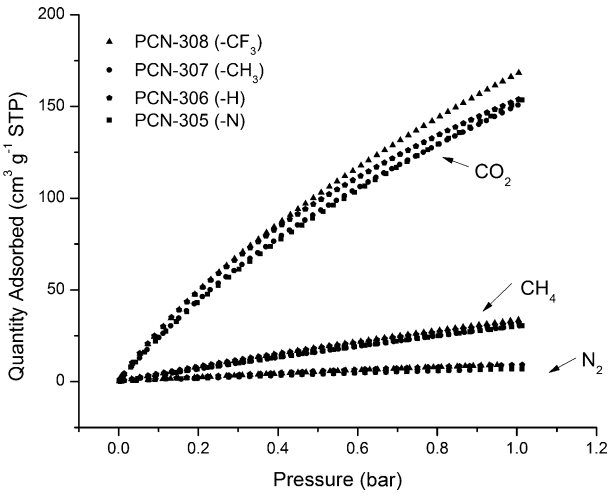

Figure 4. Sorption isotherms for CO_2, CH_4, and N_2 at 273 K of the isostructural MOFs.

Table 2. CO_2-uptake capacity at 1 bar, heat of adsorption (Q_{st}), and gas selectivities at 273 K for the isostructural MOFs.

	CO_2 uptake [wt%] at		Q_{st}	Selectivity	
	273 K	297 K	[kJ mol^{-1}]	CO_2/N_2 0.15:0.85 v/v	CO_2/CH_4 1:1 v/v
PCN-305 (−N)	23.2	14.5	23.847	52	7.2
PCN-306 (−H)	22.9	13.8	23.997	40	7.5
PCN-307 (−CH_3)	23.2	14.4	22.836	50	8.8
PCN-308 (−CF_3)	24.8	15.4	22.215	37	7.8

Table 3. CO_2-uptake capacities for MOFs at 1 bar.[a]

MOF	Capacity [wt%][b]	T [K]	Ref.
SNU-5	38.5	273	[22]
$Cu_2(EBTC)(H_2O)_2 \cdot xG$	25.9	273	[23]
Mg–MOF-74	35.2	296	[24]
HKUST-1 (4 wt% H_2O)	27	298	[25]
Cu(Me-4py-trz-ia)	26.8	298	[26]
Cu–TDPAT	25.8	298	[7d]
Co–MOF-74	24.9	298	[27]
Ni–MOF-74	23.9	298	[27]
$Cu(bpy\text{-}1)_2(SiF_6)$	23.1	298	[9]
$\{[CuL]uLLERLI_2O\}_n$	22.01	298	[28]
Zn–MOF-74	19.8	296	[27]
HKUST-1	19.8	293	[29]
MMPF-2	19.8	298	[30]
PCN-124	18.3	295	[31]
PCN-26-ac	17.6	298	[32]
HKUST-1 (8 wt% H_2O)	17.4	298	[25]
PCN-6	15.9	298	[33]
mmen–Cu–BTTri	15.4	298	[7f]

[a] EBTC = 1,1′-ethynebenzene-3,3′,5,5′-tetracarboxylate; G = guest molecule. [b] Capacities listed are the highest reported CO_2 capacities for each MOF.

face area: 1418 m^2 g^{-1}) than mmen–CuBTTri (BET surface area: 870 m^2 g^{-1}). The combined high surface area, open dicopper paddlewheel metal sites, and polar functional groups make PCN-308 a good sorbent candidate for CO_2 capture and storage.

From the adsorption isotherms, the isostructural MOFs do not show a large difference in CO_2-adsorption capacity at 1 bar. PCN-308 with polar −CF_3 functional groups has slightly higher CO_2 uptake than the other three MOFs, even though it has reduced surface area. This demonstrated that polar groups could enhance CO_2 adsorption.[8] The insignificant increase might be attributable to the decreased surface area of the framework by the addition of the functional groups. The combined effect of surface area and polar groups resulted in the slight increase in the CO_2 adsorption. However, adding methyl or pyridyl functional groups into the MOF does not change the adsorption amount. In summary, functional groups present in this structure do not have noticeable effect on the CO_2-adsorption capacity.

To better understand the adsorption properties of different functionalized MOFs, the isosteric heats of adsorption (Q_{st}) were calculated from the CO_2-adsorption isotherms at three different temperatures (273, 283, and 297 K) by using the Clausius–Clapeyron equation[21] $Q_{st} = -Rd(\ln P)/d(1/T)$ (R = gas constant, P = pressure, T = temperature; for details, see the Supporting Information). There is no significant difference in the heat of adsorption for the isostructural MOFs. It demonstrates that different functional groups in this structure do not affect the CO_2 affinity of the framework significantly.

The selectivities of CO_2/N_2 and CO_2/CH_4 were calculated from the experimental single-component isotherms by using the ideal adsorbed solution theory (IAST) method[34] (for details, see the Supporting Information). The CO_2/N_2 selectivity calculation was based on a CO_2/N_2 mixture with CO_2 concentration of 15% (partial pressure of 0.15 atm) at a total pressure of 1 atm, whereas the CO_2/CH_4 selectivity calculation was based on a CO_2/CH_4 mixture with CO_2 concentration of 50% (partial pressure of 0.50 atm) at a total pressure of 1 atm (Figure 5). The selectivities suggested by IAST

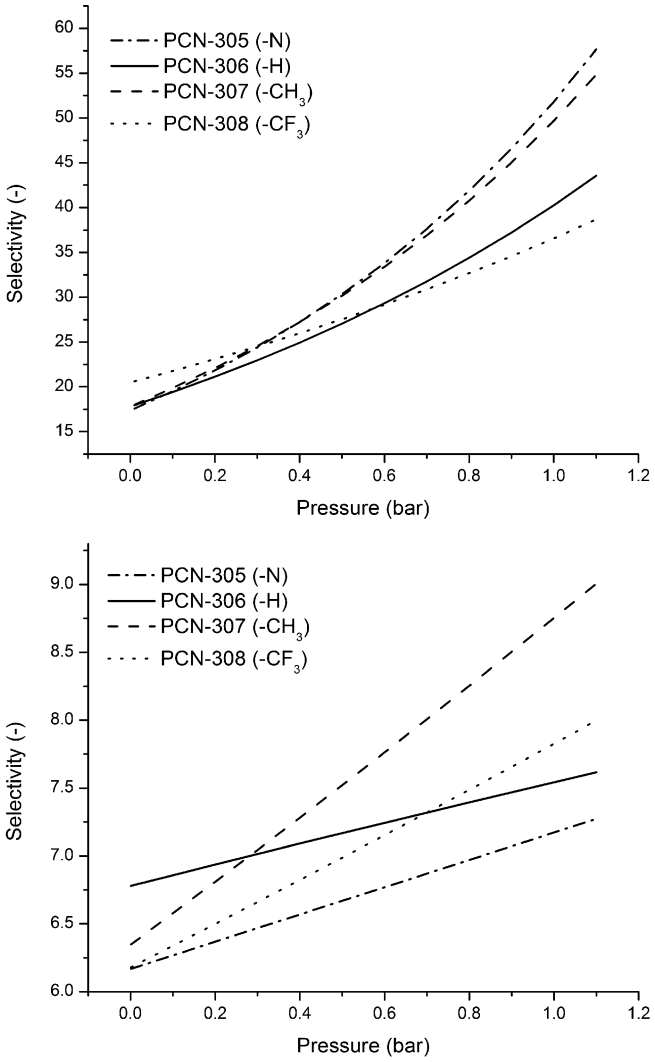

Figure 5. IAST selectivities of a) CO_2 over N_2 for 15% CO_2, 85% N_2 binary mixtures and b) CO_2 over CH_4 for equimolar binary mixtures in PCN-305, -306, -307, and -308.

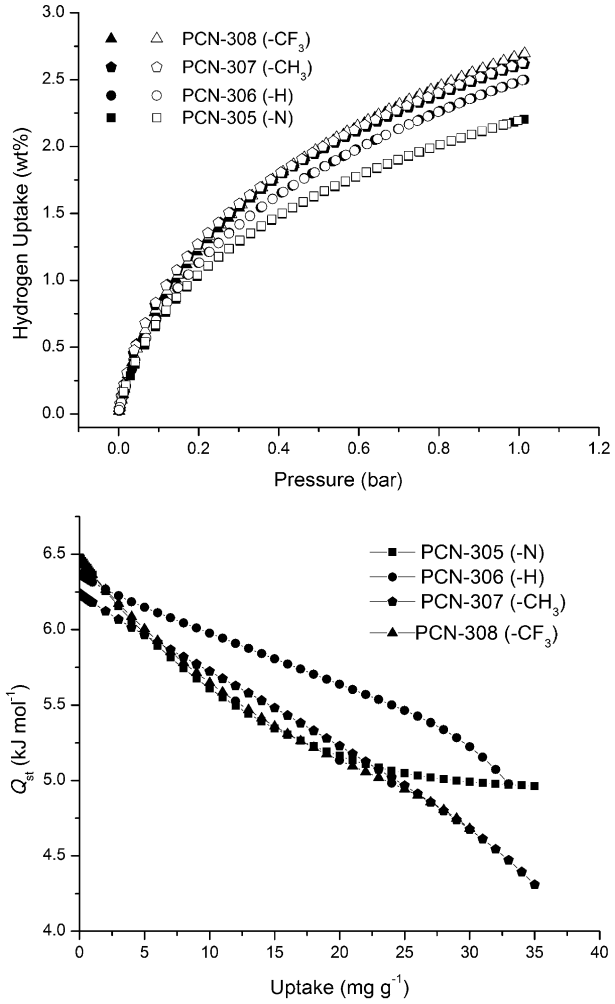

Figure 6. a) H_2 uptake and b) isosteric heats of H_2 adsorption (Q_{st}) for the isostructural MOFs.

are listed in Table 2. The isostructural MOFs showed noticeable selectivity of CO_2 over CH_4 and N_2 at 273 K. PCN-305 with pyridyl functional groups has the highest selectivity of CO_2 over N_2, whereas PCN-307 with methyl groups has the highest selectivity of CO_2 over CH_4. There is no apparent relationship between the selectivities and different functional groups in these isostructural MOFs.

H_2 uptake: Low-pressure H_2-sorption isotherms at 77 K were collected for the isostructural MOFs to evaluate their H_2-adsorption performances. They exhibited high H_2-adsorption capacity at low pressure (1 bar; Figure 6a). Among them, PCN-308 with $-CF_3$ functional groups exhibits a hydrogen uptake of 2.67 wt% at 1 bar and 77 K, which is among the highest for MOFs at low pressure. There are only six reported MOFs that have higher hydrogen uptake than PCN-308 at 1 bar and 77 K as listed in Table 4. As shown, although PCN-308 has a lower surface area than PCN-14,[35] the hydrogen uptake does not drop significantly, which might be attributed to the high density of unsaturated open metal sites after activation. PCN-12, which was reported by the same group, has the second-highest hydrogen uptake so far. It was also constructed from ligands with two isophthlate moieties (methylenediisophthalate (mdip)). But unlike the 1D channel structure in the isostructural MOFs reported in this work, the isophthalate moieties in the mdip ligand formed cuboctahedral cages. This was because in the mdip ligand, the two isophthalate groups are linked by a bent bridge (methylene) instead of the rigid benzene ring in this work. Their structural difference results in the difference in gas-sorption properties.

The isosteric heats of adsorption were calculated on the basis of the H_2-adsorption isotherms at 77 and 87 K for each compound (Figure 6b). The functional groups did not show significant influence in either the H_2 uptake or the heat of adsorption. It demonstrated that for these isostructural MOFs the capacity of hydrogen is basically related to the structures. Different functional groups have little effect on the H_2 uptake.

Conclusion

A series of robust, porous, isostructural MOFs with different functional groups have been synthesized from diisophthalate ligands on the basis of a ligand-truncation strategy. The frameworks adopt a unique 4-c 4-nodal net topology with the Schlafli symbol of $\{4.6^4.8\}_2\{4^2.6^4\}\{6^4.8^2\}_2\{6^6\}$. The isostructural MOFs showed not only high CO_2-adsorption capacities but also noticeable selectivities of CO_2 over CH_4 and N_2. Moreover, they exhibited high H_2 uptake, particularly for PCN-308 with $-CF_3$ functional group (2.67 wt% at 77 K/1 bar). For the series of isostructural MOFs, the capacities of CO_2 and H_2 are basically related to the textural properties rather than the functional groups of the MOFs.

Table 4. H_2 uptake and heat of adsorption for selected MOFs and PCN-305, -306, -307, and -308.

	S_{BET} [m^2g^{-1}]	$S_{Langmuir}$ [m^2g^{-1}]	H_2 uptake [wt%]	Q_{st} [$kJmol^{-1}$]	Ref.
PCN-12	1943	2425	3.05		[26]
UTSA-20	1156		2.9		[27]
SNU-5		2850	2.84		[28]
$Cu_4(TTPM)_2{\cdot}0.7\,CuCl_2$	2506	2745	2.8		[29]
PCN-14	1753		2.7	8.6	[25]
PCN-308	1418.66	2234.21	2.67	6.48	this work
PCN-307	1376.68	2235.89	2.62	6.24	this work
PCN-306	1927.44	2929.19	2.50	6.37	this work
PCN-305	1650.75	2550.25	2.20	6.47	this work

Experimental Section

Materials and methods: All the general reagents were commercially available and used as received. $Cu(NO_3)_2{\cdot}2.5H_2O$ was purchased from VWR; 1,3-dibromobenzene from Alfa Aesar; 3,5-dibromotoluene from TCI America; 3,5-dibromopyridine from Frontier Scientific; and 3,5-dibromobenzotrifluoride from AOBChem. Dimethyl 5-(4,4,5,5-tetramethyl-1,3,2-dioxaborolan-2-yl)isophthalate and diethyl 5-(4,4,5,5-tetramethyl-1,3,2-dioxaborolan-2-yl)isophthalate[36] were synthesized according to reported procedures. ^{1}H NMR spectroscopic data was collected using a Mercury 300 spectrometer. Elemental microanalyses (EA) were performed by Atlantic Microlab, Inc. FTIR data were recorded using an IRAffinity-1 instrument. TGA data were obtained using a TGA-50 (Shimadzu) thermogravimetric analyzer with a heating rate of 2 °C min^{-1} under an N_2 atmosphere. The PXRD patterns were recorded using a Bruker D8-Focus Bragg–Brentano X-ray powder diffractometer equipped with a Cu sealed tube ($\lambda = 1.54178$ Å) at room temperature. Simulation of the PXRD spectrum was carried out by the single-crystal data and the diffraction-crystal module of the *Mercury* program available free of charge on the Internet.

Synthesis of [1,1′:3′,1″-terphenyl]-3,3″,5,5″-tetracarboxylic acid (H_4TPTA): 1,3-Dibromobenzene (1.00 g, 4.24 mmol), dimethyl 5-(4,4,5,5-tetramethyl-1,3,2-dioxaborolan-2-yl)isophthalate (3.00 g, 9.33 mmol), CsF (4.00 g), and $[Pd(PPh_3)_4]$ (200 mg) were added to a 250 mL Schlenk flask. The flask was connected to Schlenk line, the air was evacuated, and then refilled with nitrogen. 1,2-Dimethoxyethane (DME; 150 mL) was degassed (2 h) and added to the flask through a cannula. The flask was equipped with a water condenser and heated to reflux under nitrogen for 3 days. The solvent was removed on a rotary evaporator. H_2O (100 mL) was added and extracted with CH_2Cl_2. The organic phase was dried with $MgSO_4$. After the removal of CH_2Cl_2 solvent, the crude product was washed with acetone to give pale yellow solid product tetraethyl [1,1′:3′,1″-terphenyl]-3,3″,5,5″-tetracarboxylate with a yield of 70% (1.54 g) based on 1,3-dibromobenzene. ^{1}H NMR (300 MHz, CD_3Cl): $\delta =$ 3.98 (s, 12H), 7.61 (t, 1H), 7.67 (d, 2H), 7.86 (t, 1H), 8.50 (d, 4H), 8.69 ppm (t, 2H).

Tetraethyl [1,1′:3′,1″-terphenyl]-3,3″,5,5″-tetracarboxylate (1.54 g) was dissolved in a mixed solvent of THF and MeOH (60 mL, 1:1 v/v), and NaOH (20 mL, 2 N) aqueous solution was added. The mixture was stirred at room temperature overnight. After the organic phase was removed, the aqueous phase was acidified with 20% hydrochloric acid to give a white precipitate, which was filtered and washed with water several times. Yield: 1.27 g, 94%. ^{1}H NMR (300 MHz, [D$_6$]DMSO): $\delta = 7.65$ (t, 1H), 7.80 (d, 2H), 8.04 (s, 1H), 8.46 ppm (s, 6H); FTIR (KBr): $\tilde{\nu} = 3017$ (w), 2633 (w), 1717 (s), 1595 (w), 1454 (m), 1415 (m), 1364 (m), 1288 (s), 1213 (s), 1118 (w), 1078 (w), 923 (m), 796 (w), 756 (s), 691 cm^{-1} (m).

Synthesis of 5,5′-(pyridine-3,5-diyl)diisophthalic acid (H_4PDDA): This was synthesized by following a similar procedure to the synthesis of ligand H_4PDDA. Except for changing the starting materials of 1,3-dibromobenzene to 3,5-dibromopyridine, the molar ratio of the reactants remained the same. Tetraethyl 5,5′-(pyridine-3,5-diyl)diisophthalate: ^{1}H NMR (300 MHz, CD_3Cl): $\delta = 1.45$ (t, 12H), 4.76 (q, 6H), 8.19 (d, 1H), 8.52 (d, 4H), 8.77 (t, 2H), 8.96 ppm (s, 2H). H_4PDDA: ^{1}H NMR (300 MHz, [D$_6$]DMSO): $\delta = 8.55$ (t, 2H), 8.61 (q, 4H), 8.79 (s, 1H), 9.12 ppm (s, 2H); FTIR (KBr): $\tilde{\nu} = 3016$ (w), 1741 (s), 1458(w), 1365 (m), 1219 (s), 1145 (w), 1066 (w), 958 (w), 894 (m), 812 (w), 758 (m), 669 cm^{-1} (w).

Synthesis of 5′-(trifluoromethyl)-[1,1′:3′,1″-terphenyl]-3,3″,5,5″-tetracarboxylic acid (H_4FTPTA): This was synthesized by following a similar procedure to the synthesis of ligand H_4PDDA. Except for changing the starting materials of 1,3-dibromobenzene to 1,3-dibromo-5-(trifluoromethyl)-benzene, the molar ratio of the reactants remained the same. Tetraethyl 5′-(trifluoromethyl)-[1,1′:3′,1″-terphenyl]-3,3″,5,5″-tetracarboxylate: ^{1}H NMR (300 MHz, CD_3Cl): $\delta = 1.42$ (t, 12H), 4.44 (q, 8H), 7.88 (s, 2H), 8.01 (s, 1H), 8.45 (d, 4H), 8.71 ppm (t, 2H). H_4FTPTA: ^{1}H NMR (300 MHz, [D$_6$]DMSO): $\delta = 8.12$ (s, 2H), 8.39 (s, 1H), 8.53 (s, 2H), 8.54 ppm (s, 4H); FTIR (KBr): $\tilde{\nu} = 3014$ (w), 2652 (w), 2558 (w), 1716 (s), 1606 (w), 1408 (m), 1356 (m), 1321 (m), 1269 (s), 1219 (w), 1188 (w), 1112 (s), 1093 (w), 914 (w), 887 (m), 758 (m), 694 (m), 665 cm^{-1} (w).

Synthesis of 5′-methyl-[1,1′:3′,1″-terphenyl]-3,3″,5,5″-tetracarboxylic acid (H_4MTPTA): This was synthesized by following a similar procedure to the synthesis of ligand H_4PDDA. Except for changing the starting materials of 1,3-dibromobenzene to 1,3-dibromo-5-methylbenzene, the molar ratio of the reactants remained the same. Tetraethyl 5′-methyl-[1,1′:3′,1″-terphenyl]-3,3″,5,5″-tetracarboxylate: ^{1}H NMR (300 MHz, CD_3Cl): $\delta =$ 1.41 (t, 12H), 2.50 (s, 3H), 4.42 (q, 8H), 7.47 (s, 2H), 7.64 (s, 1H), 8.44 (d, 4H), 8.71 ppm (t, 2H). H_4MTPTA: ^{1}H NMR (300 MHz, [D$_6$]DMSO): $\delta = 2.30$ (s, 3H), 7.64 (d, 2H), 7.84 (s, 1H), 8.46 (q, 6H); FTIR (KBr): $\tilde{\nu} = 2989$ (w), 2650 (w), 2579 (w), 1728 (s), 1595 (w), 1450 (m), 1359 (m), 1288 (m), 1213 (s), 1143 (w), 1085 (w), 920 (w), 862 (w), 760 (s), 705 (m), 673 cm^{-1} (m).

Synthesis of PCN-305: A solution of ligand H_4PDDA (80 mg, 0.20 mmol), $Cu(NO_3)_2{\cdot}2.5H_2O$ (160 mg, 0.85 mmol), and tetrafluoroboric acid (HBF_4; 0.2 mL, 48% w/w aqueous solution) in *N*,*N*-dimethylacetamide (DMA; 17 mL) was sealed in a 20 mL glass vial and placed in an oven at 75 °C. Blue block crystals that were suitable for X-ray analysis formed within 72 h. FTIR (KBr): $\tilde{\nu} = 3446$ (w), 2934 (w), 1664 (s), 1507 (w), 1395 (s), 1250 (w), 1103 (m), 1024 (m), 958 (w), 859 (w), 773 (m), 729 (s), 662 cm^{-1} (m).

Synthesis of PCN-306: A solution of ligand H_4TPTA (80 mg, 0.20 mmol), $Cu(NO_3)_2{\cdot}2.5H_2O$ (160 mg, 0.85 mmol), and tetrafluoroboric acid (HBF_4; 0.1 mL, 48% w/w aqueous solution) in DMF (17 mL) was sealed in a 20 mL glass vial and placed in an oven at 60 °C. Blue crystalline powder was obtained within 72 h. FTIR (KBr): $\tilde{\nu} = 3305$ (w), 2603 (w), 1861 (w), 1718 (m), 1610 (m), 1550 (s), 1423 (m), 1366 (s), 1225 (m), 1151 (w), 1128 (w), 1072 (w), 922 (w), 896 (w), 773 (s), 719 (m), 702 cm^{-1} (w).

Synthesis of PCN-307: Carried out by following the same procedure as that for **PCN-306**. A solution of ligand H_4MTPTA (80 mg, 0.19 mmol), $Cu(NO_3)_2{\cdot}2.5H_2O$ (160 mg, 0.85 mmol), and tetrafluoroboric acid (HBF_4; 0.1 mL, 48% w/w aqueous solution) in DMF (17 mL) was sealed in a 20 mL glass vial and placed in an oven at 60 °C. Blue crystalline powder was obtained within 72 h. FTIR (KBr): $\tilde{\nu} = 3063$ (w), 2380 (w), 1715 (m), 1628 (m), 1562 (s), 1418 (s), 1375 (s), 1280 (m), 1219 (m), 1128 (w), 1082 (w), 885 (w), 775 (m), 732 (m), 683 (w), 669 cm^{-1} (w).

Synthesis of PCN-308: Carried out by following the same procedure as that for **PCN-306**. A solution of ligand H_4FTPTA (80 mg, 0.17 mmol), $Cu(NO_3)_2{\cdot}2.5H_2O$ (160 mg, 0.85 mmol), and tetrafluoroboric acid (HBF_4; 0.1 mL, 48% w/w aqueous solution) in DMF (17 mL) was sealed in a 20 mL glass vial and placed in an oven at 60 °C. Blue crystalline powder was obtained within 72 h. FTIR (KBr): $\tilde{\nu} = 3092$ (w), 2374 (w), 1701 (w), 1618 (m), 1560 (s), 1413 (s), 1352 (s), 1276 (m), 1176 (w), 1116 (m), 1082 (w), 891 (m), 763 (m), 723 (m), 650 cm^{-1} (w).

Crystal data for PCN-305 [Cu_2(PDDA)]: $C_{63}H_{24}Cu_6N_3O_{30}$; $M_r = 1684.15$; orthorhombic; $a = 24.650(7)$, $b = 33.494(9)$, $c = 18.529(5)$ Å; $V =$ 15298.04 Å^3; $T = 110(2)$ K; space group *Cmcm*; $Z = 4$; $R_{int} = 0.1109$; $R_1 =$ 0.1371; $wR_2 = 0.4164$; GoF = 0.999.

CCDC-900615 (**PCN-305**) contains the supplementary crystallographic data for this paper. These data can be obtained free of charge from The Cambridge Crystallographic Data Centre via www.ccdc.cam.ac.uk/data_request/cif.

Acknowledgements

This work was supported as part of the Center for Gas Separations Relevant to Clean Energy Technologies, an Energy Frontier Research Center funded by the U.S. Department of Energy (DOE), Office of Science, Office of Basic Energy Sciences under Award Number DE-SC0001015.

[1] a) J.-R. Li, Y. Ma, M. C. McCarthy, J. Sculley, J. Yu, H.-K. Jeong, P. B. Balbuena, H.-C. Zhou, *Coord. Chem. Rev.* **2011**, *255*, 1791; b) Y. Liu, Z. U. Wang, H.-C. Zhou, *Greenhouse Gases: Science and*

Technology **2012**, *2*, 239; c) K. Sumida, D. L. Rogow, J. A. Mason, T. M. McDonald, E. D. Bloch, Z. R. Herm, T.-H. Bae, J. R. Long, *Chem. Rev.* **2011**, *111*, 724; d) J. Liu, P. K. Thallapally, B. P. McGrail, D. R. Brown, J. Liu, *Chem. Soc. Rev.* **2012**, *41*, 2308; e) Y.-S. Bae, R. Q. Snurr, *Angew. Chem.* **2011**, *123*, 11790; *Angew. Chem. Int. Ed.* **2011**, *50*, 11586; f) G. Férey, C. Serre, T. Devic, G. Maurin, H. Jobic, P. L. Llewellyn, G. De Weireld, A. Vimont, M. Daturi, J.-S. Chang, *Chem. Soc. Rev.* **2011**, *40*, 550.

[2] a) M. Eddaoudi, D. B. Moler, H. Li, B. Chen, T. M. Reineke, M. O'Keeffe, O. M. Yaghi, *Acc. Chem. Res.* **2001**, *34*, 319; b) O. M. Yaghi, M. O'Keeffe, N. W. Ockwig, H. K. Chae, M. Eddaoudi, J. Kim, *Nature* **2003**, *423*, 705; c) H.-C. Zhou, J. R. Long, O. M. Yaghi, *Chem. Rev.* **2012**, *112*, 673; d) J. J. Perry Iv, J. A. Perman, M. J. Zaworotko, *Chem. Soc. Rev.* **2009**, *38*, 1400; e) M. O'Keeffe, O. M. Yaghi, *Chem. Rev.* **2011**, *111*, 675.

[3] a) M. Dincă, J. R. Long, *Angew. Chem.* **2008**, *120*, 6870; *Angew. Chem. Int. Ed.* **2008**, *47*, 6766; b) S. Ma, H.-C. Zhou, *J. Am. Chem. Soc.* **2006**, *128*, 11734.

[4] a) K. K. Tanabe, S. M. Cohen, *Chem. Soc. Rev.* **2011**, *40*, 498; b) S. M. Cohen, *Chem. Rev.* **2011**, *111*, 970; c) S. Kitagawa, R. Kitaura, S.-i. Noro, *Angew. Chem.* **2004**, *116*, 2388; *Angew. Chem. Int. Ed.* **2004**, *43*, 2334.

[5] J. L. C. Rowsell, O. M. Yaghi, *Angew. Chem.* **2005**, *117*, 4748; *Angew. Chem. Int. Ed.* **2005**, *44*, 4670.

[6] a) D. Sun, S. Ma, Y. Ke, D. J. Collins, H.-C. Zhou, *J. Am. Chem. Soc.* **2006**, *128*, 3896; b) B. Panella, M. Hirscher, H. Pütter, U. Müller, *Adv. Funct. Mater.* **2006**, *16*, 520; c) X.-S. Wang, S. Ma, D. Yuan, J. W. Yoon, Y. K. Hwang, J.-S. Chang, X. Wang, M. R. Jørgensen, Y.-S. Chen, H.-C. Zhou, *Inorg. Chem.* **2009**, *48*, 7519; d) J. Sculley, D. Yuan, H.-C. Zhou, *Energy Environ. Sci.* **2011**, *4*, 2721; e) M. P. Suh, H. J. Park, T. K. Prasad, D.-W. Lim, *Chem. Rev.* **2011**, *111*, 782.

[7] a) Y. Zou, M. Park, S. Hong, M. S. Lah, *Chem. Commun.* **2008**, 2340; b) B. Zheng, J. Bai, J. Duan, L. Wojtas, M. J. Zaworotko, *J. Am. Chem. Soc.* **2010**, *132*, 748; c) R. Luebke, J. F. Eubank, A. J. Cairns, Y. Belmabkhout, L. Wojtas, M. Eddaoudi, *Chem. Commun.* **2012**, *48*, 1455; d) B. Li, Z. Zhang, Y. Li, K. Yao, Y. Zhu, Z. Deng, F. Yang, X. Zhou, G. Li, H. Wu, N. Nijem, Y. J. Chabal, Z. Lai, Y. Han, Z. Shi, S. Feng, J. Li, *Angew. Chem. Int. Ed.* **2012**, *51*, 1412; e) T. M. McDonald, W. R. Lee, J. A. Mason, B. M. Wiers, C. S. Hong, J. R. Long, *J. Am. Chem. Soc.* **2012**, *134*, 7056; f) T. M. McDonald, D. M. D'Alessandro, R. Krishna, J. R. Long, *Chem. Sci.* **2011**, *2*, 2022; g) R. Vaidhyanathan, S. S. Iremonger, G. K. H. Shimizu, P. G. Boyd, S. Alavi, T. K. Woo, *Science* **2010**, *330*, 650; h) J. An, S. J. Geib, N. L. Rosi, *J. Am. Chem. Soc.* **2009**, *131*, 38; i) J. An, N. L. Rosi, *J. Am. Chem. Soc.* **2010**, *132*, 5578.

[8] Y.-S. Bae, O. K. Farha, J. T. Hupp, R. Q. Snurr, *J. Mater. Chem.* **2009**, *19*, 2131.

[9] S. D. Burd, S. Ma, J. A. Perman, B. J. Sikora, R. Q. Snurr, P. K. Thallapally, J. Tian, L. Wojtas, M. J. Zaworotko, *J. Am. Chem. Soc.* **2012**, *134*, 3663.

[10] C. Yang, X. Wang, M. A. Omary, *J. Am. Chem. Soc.* **2007**, *129*, 15454.

[11] C. Zlotea, D. Phanon, M. Mazaj, D. Heurtaux, V. Guillerm, C. Serre, P. Horcajada, T. Devic, E. Magnier, F. Cuevas, G. Ferey, P. L. Llewellyn, M. Latroche, *Dalton Trans.* **2011**, *40*, 4879.

[12] H. K. Chae, D. Y. Siberio-Perez, J. Kim, Y. Go, M. Eddaoudi, A. J. Matzger, M. O'Keeffe, O. M. Yaghi, *Nature* **2004**, *427*, 523.

[13] D. Yuan, D. Zhao, D. Sun, H.-C. Zhou, *Angew. Chem.* **2010**, *122*, 5485; *Angew. Chem. Int. Ed.* **2010**, *49*, 5357.

[14] D. Zhao, D. Yuan, D. Sun, H.-C. Zhou, *J. Am. Chem. Soc.* **2009**, *131*, 9186.

[15] D. Sun, Y. Ke, T. M. Mattox, S. Parkin, H.-C. Zhou, *Inorg. Chem.* **2006**, *45*, 7566.

[16] S. R. Batten, R. Robson, *Angew. Chem.* **1998**, *110*, 1558; *Angew. Chem. Int. Ed.* **1998**, *37*, 1460.

[17] A. P. Nelson, O. K. Farha, K. L. Mulfort, J. T. Hupp, *J. Am. Chem. Soc.* **2008**, *130*, 458.

[18] P. Zhang, B. Li, Y. Zhao, X. Meng, T. Zhang, *Chem. Commun.* **2011**, *47*, 7722.

[19] A. Spek, *J. Appl. Crystallogr.* **2003**, *36*, 7.

[20] W. Lu, D. Yuan, T. A. Makal, J.-R. Li, H.-C. Zhou, *Angew. Chem. Int. Ed.* **2012**, *51*, 1580.

[21] F. Rouquerol, J. Rouquerol, J. Sing, *Adsorption by Powders and Porous Solids: Principles, Methodology, and Applications*, Academic Press, London, **1999**.

[22] Y.-G. Lee, H. R. Moon, Y. E. Cheon, M. P. Suh, *Angew. Chem.* **2008**, *120*, 7855; *Angew. Chem. Int. Ed.* **2008**, *47*, 7741.

[23] Y. Hu, S. Xiang, W. Zhang, Z. Zhang, L. Wang, J. Bai, B. Chen, *Chem. Commun.* **2009**, 7551.

[24] S. R. Caskey, A. G. Wong-Foy, A. J. Matzger, *J. Am. Chem. Soc.* **2008**, *130*, 10870.

[25] A. O. Yazaydın, A. I. Benin, S. A. Faheem, P. Jakubczak, J. J. Low, R. R. Willis, R. Q. Snurr, *Chem. Mater.* **2009**, *21*, 1425.

[26] D. Lässig, J. Lincke, J. Moellmer, C. Reichenbach, A. Moeller, R. Gläser, G. Kalies, K. A. Cychosz, M. Thommes, R. Staudt, H. Krautscheid, *Angew. Chem.* **2011**, *123*, 10528; *Angew. Chem. Int. Ed.* **2011**, *50*, 10344.

[27] A. O. Yazaydın, R. Q. Snurr, T.-H. Park, K. Koh, J. Liu, M. D. LeVan, A. I. Benin, P. Jakubczak, M. Lanuza, D. B. Galloway, J. J. Low, R. R. Willis, *J. Am. Chem. Soc.* **2009**, *131*, 18198.

[28] L. Wen, W. Shi, X. Chen, H. Li, P. Cheng, *Eur. J. Inorg. Chem.* **2012**, *2012*, 3562.

[29] P. Aprea, D. Caputo, N. Gargiulo, F. Iucolano, F. Pepe, *J. Chem. Eng. Data* **2010**, *55*, 3655.

[30] X.-S. Wang, M. Chrzanowski, C. Kim, W.-Y. Gao, L. Wojtas, Y.-S. Chen, X. P. Zhang, S. Ma, *Chem. Commun.* **2012**, *48*, 7173.

[31] J. Park, J.-R. Li, Y.-P. Chen, J. Yu, A. A. Yakovenko, Z. U. Wang, L.-B. Sun, P. B. Balbuena, H.-C. Zhou, *Chem. Commun.* **2012**, *48*, 9995.

[32] W. Zhuang, D. Yuan, D. Liu, C. Zhong, J.-R. Li, H.-C. Zhou, *Chem. Mater.* **2011**, *23*, 18.

[33] J. Kim, S.-T. Yang, S. B. Choi, J. Sim, J. Kim, W.-S. Ahn, *J. Mater. Chem.* **2011**, *21*, 3070.

[34] a) Y.-S. Bae, O. K. Farha, A. M. Spokoyny, C. A. Mirkin, J. T. Hupp, R. Q. Snurr, *Chem. Commun.* **2008**, 4135; b) Y.-S. Bae, K. L. Mulfort, H. Frost, P. Ryan, S. Punnathanam, L. J. Broadbelt, J. T. Hupp, R. Q. Snurr, *Langmuir* **2008**, *24*, 8592; c) M. Heuchel, R. Q. Snurr, E. Buss, *Langmuir* **1997**, *13*, 6795; d) A. L. Myers, J. M. Prausnitz, *AIChE J.* **1965**, *11*, 121.

[35] S. Ma, J. M. Simmons, D. Sun, D. Yuan, H.-C. Zhou, *Inorg. Chem.* **2009**, *48*, 5263.

[36] J. Natera, L. Otero, L. Sereno, F. Fungo, N.-S. Wang, Y.-M. Tsai, T.-Y. Hwu, K.-T. Wong, *Macromolecules* **2007**, *40*, 4456.

Received: September 14, 2012
Revised: January 17, 2013
Published online: February 27, 2013

